8-5-2014

Constructing Water Budgets for a Coastal Stormwater Catchment to Examine Temporal Dynamics Between Urban Groundwater and Surface Runoff

Leigha E. Peterson
Coastal Carolina University

CONSTRUCTING WATER BUDGETS FOR A COASTAL STORMWATER CATCHMENT TO EXAMINE TEMPORAL DYNAMICS BETWEEN URBAN GROUNDWATER AND SURFACE RUNOFF

Leigha E. Peterson

Submitted in Partial Fulfillment of the
Requirements for the Degree of Master of Science in
Coastal Marine and Wetland Studies in the
College of Science
Coastal Carolina University
2014

Dr. Richard N. Peterson
Dr. Erik Smith
Dr. Richard F. Viso
Dr. Susan Libes

August 5, 2014
Conway, South Carolina

Acknowledgements

This work would have not exist if not for the assistance and guidance of many individuals directly involved and otherwise. Most notably, my thesis advisor, Dr. Rick Peterson, for invaluable science and life lessons. Hats off to you, Rick. I look forward to the next few years! Thank you to Dr. Rich Viso, Dr. Erik Smith, and Dr. Susan Libes for your assistance in the thesis production. Each of you has offered invaluable insight through this process and facilitated the development of the Swash Project and this manuscript. The author would like to extend many thanks to the agencies whom supported this work: NOAA/NEERs Science Collaborative (Award 11-037), the Slocum-Lunz Foundation, M.K. Pentecost Ecology Fund, Horry County, and the City of Myrtle Beach.

To members of the Groundwater Discharge Measurement Facility at Coastal Carolina University: I have never met such a fun, talented, and supportive group of individuals. Thank you and good luck to you all–members past, present, and future. A special and sincere thanks to Chris 'Carl' Mchugh, Matt Carter, Sarah Chappel, Patrick Hutchins, Kelly Nifong, Brian Johnson, Dr. Jenna Hill, Shinobu Okano, Jamie Brusa, Brad Craig, Rohen Gresalfi, and Sam Maness for field assistance, assisting in data collection and interpretations, and positive attitudes! Angie Defore, you have been a pleasure to work with, I hope our paths cross again. Thank you also to United States Geological Survey employees Victor Levesque and Jeremy Pulli for the hours of assistance and patience.

Lastly, thank you to my mother. You are undoubtedly the strongest person I know and a great model to follow. You have pushed and encouraged me always. Thank you for showing me regardless of the weather, I can always have sunshine. I will take it with me always.

Abstract

It is well understood that urbanization results in changes to the hydrologic cycle, namely increasing surface runoff production rates. Precipitation falling on impervious areas is typically directed via a network of drainage pipes to detention reservoirs, a process shown to negatively impact aquifer recharge rates. Historically, urban hydrologists have focused primarily on surface processes with little consideration to subsurface implications of the urban water cycle. Here, we present an approach to construct long-term, high-resolution water budgets for a coastal stormwater catchment resolving surface runoff and groundwater fractions within the water body and associated source-specific fluid exports to the coastal ocean. We use the radiotracer ^{222}Rn to delineate groundwater fraction within the reservoir, calculate direct precipitation inputs, and by difference, determine surface runoff contributions to the total water budget. By determining total output rates from Dogwood Swash, we also examine relative source outputs at both high- and low-resolution temporal scales from 2012 through 2013. While surface runoff constituted the majority of the water budget, both groundwater and surface runoff fractions varied by 36.5% suggesting the subsurface source to contribute significantly to the stormwater catchment fluid budget. However, long-term records indicate a decline in groundwater fraction (by 35%) and export (14%) from the system as aquifer residence times increased. Constructing water budgets for sub-basin tributaries within the larger Dogwood Swash drainage complex suggest reduced source water variability, lower groundwater fractions, and longer aquifer residence times with greater impervious surface area. Our approach to water budget construction may be applied to other environments providing the framework for source-specific material budgets. Such assessments could then be used by stormwater managers to best maintain desired ecosystem health in both urban streams and the coastal ocean.

Table of Contents

List of Tables

List of Figures

Introduction

Anthropogenic landscape alterations due to urbanization can significantly alter the fate of precipitation by preventing those waters from infiltrating into shallow aquifers, instead being redirected through overland flowpaths. In urban areas, stormwater conveyance systems are engineered to rapidly transport water away from roads, parking lots, and buildings such that the rate of fluid delivery to receiving waters is increased (Booth and Jackson, 1997). Waters of either surface or subsurface origin deliver material loads to neighboring water bodies based on their unique transit pathways and transport times (Loucaides et al., 2007; Hildebrandt et al., 2008). Changes in material load (quality and quantity) as well as delivery rate (e.g., dosage) in turn may yield biological shifts with potentially whole-scale ecological ramifications (Booth et al., 2002; Hancock et al., 2005).

Historically, impervious surfaces have been believed to convert 100% of precipitation to overland flow thus completely negating infiltration processes in urban areas (e.g., Johnson and Sayre 1973). For this reason, much of the urban hydrology literature is surface runoff centric, focusing primarily on hydrographic concepts (Meriano et al., 2011), urban channel geomorphology (Vietz et al., 2014), and ecological responses (Grimm et al., 2008). A review by Brabec et al. (2002) reveals most urban watershed work has focused on physical, chemical, and biological stream health parameters with little regard to fluid origin as the cause of degraded urban water quality. Since the review by Brabec et al. (2002), researchers have begun to investigate fluid sources to urban streams and examine associated water balances (Haase 2009). With advancements in hydrologic simulations, researches have incorporated complex surface and subsurface interactions (Arnold and Allen 1996; Arnold et al., 2000) able to hindcast pre-developed hydraulic conditions and compare them to current or forecasted urbanized hydraulic

regimes to assess the role of development in urban fluid dynamics (Barron et al., 2013). Such modeling efforts require field measurements for calibration/validation to generate realistic results.

To date, however, measurements of groundwater fluxes to urban systems have primarily relied upon indirect approaches (e.g., water balance differences and hydrograph separation) to constrain this often difficult to measure water source component (e.g., Hasse 2009; Meriano et al., 2011). Recently, more direct methods have been developed to quantify groundwater fluxes to water bodies including seepage meters and natural geochemical tracers (e.g., Ra isotopes, ^{222}Rn, CH_4, U isotopes, and C isotopes). Many of the studies exercising these newer techniques have focused attention on inputs to the coastal ocean (Burnett et al., 2006), rivers (Mullinger et al., 2007), estuaries (Santos et al., 2010), and lakes (Dimova and Burnett 2011) in rural and suburban settings rather than confined urban water bodies. In coastal urbanized settings, source delineation is essential as waters are transported offshore influencing not only the urban stream, but also the coastal ocean with unique biological implications to each environment (Hutchins et al., 2014).

To understand how hydrologic changes impact receiving waters, we must understand relative fluid contributions from both surface and subsurface sources to discern source-specific material loads to urban water bodies and the coastal ocean. In this study, we construct long-term, high-resolution water budgets for a coastal stormwater catchment to examine fluid contributions within the catchment and quantify source-specific system outputs. In constraining temporal surface runoff and groundwater source dynamics, we hypothesize surface runoff will constitute the majority of the water budget in this urban setting with unique fluctuations in groundwater contributions on seasonal and event-driven scales related to rainfall patterns. The objectives of this study are to: 1) construct long-term quantitative total discharge rate records for an urban

stream; 2) assemble time-series water budgets for the system by resolving groundwater fractions, computing direct precipitation fractions, and determining surface runoff fractions by difference; and 3) calculate source-specific outputs from the coastal drainage canal to quantify that which enters the neighboring coastal ocean. These water budgets and associated source-specific flux records will be used in a follow-up study to assess the role of surface and subsurface flowpaths on nutrient biogeochemical cycling within the urban stream and resulting fluxes to the coastal ocean.

Methods

Geographic Setting and Site Descriptions

The Grand Strand is a stretch of semi-contiguous shoreline from Winyah Bay to Little River along the northern coastline of South Carolina. This region includes approximately 100 km of beaches and supports over fourteen million seasonal tourists each year. Extensive development in the Grand Strand and surrounding coastal towns has led to the need to transmit stormwater runoff offshore, effectively resulting in intense engineered water conveyance systems. One technique employed in this region is to collect stormwater runoff from pipes, ditches, and detention ponds into conveyance creeks (locally known as 'swashes'), which traverse the beach and discharge into neighboring marine waters, Long Bay. A total of fifteen of these swashes exist throughout the Grand Strand, and range from non-tidal (e.g., weired near the outlet) to fully tidally flushed. Swash waters are open to the atmosphere (accumulating direct precipitation along the flowpath) and flow across permeable sediments (allowing exchange of groundwater through transport) providing an environment for internal transformations of nutrients, metals, bacteria, and pollutants in transit through developed lands.

Results from Hutchins et al. (2014) demonstrate the relation between urban development, surface and subsurface water quality, and resulting microbial activity in shallow aquifers. More specifically, the pristine and developed environments investigated by Hutchins et al. (2014) can be most notably characterized by extreme differences in the area of impervious cover and land use between sites, two variables intimately influencing hydrologic processes (e.g., infiltration of rainwater, magnitude of surface runoff, and subsequent discharge rates of both surface and subsurface sources). To further develop the concepts outlined by Hutchins et al. (2014), we collected long-term, high-resolution hydrologic records from Dogwood Swash, a non-tidal

conveyance creek of the Grand Strand, specifically investigating source water dynamics over annual, seasonal, and weekly (e.g., storm/drought periods) temporal scales. We supplement our interpretations regarding the relationship between source water ratios (e.g., surface: subsurface water fraction ratios) and total discharge from the swash by examining three upstream tributaries within the drainage basin, each sub-basin comprised of unique combinations of impervious cover and land use practices, to assess local heterogeneity of land use to surface and subsurface hydrology. To examine the potential influence of land use on source water ratios to Dogwood Swash and its tributaries, we developed a classification scheme considering predominant activities, ultimately categorizing impervious vs. pervious area. Using aerial imagery, GIS tools, and our classification guidelines, we digitized each basin to quantify total area of each activity and that of impervious cover.

Dogwood Swash

Dogwood Swash discharges into Long Bay through the town of Surfside Beach, draining ~4.7 km^2 of forested uplands and developed regions of variable functions and densities. The Dogwood Swash drainage basin is characterized by low relief topography and includes mostly residential, recreational, and municipal development categories, as well as undeveloped forested regions. Developed lands account for 65% of the total basin area, with vegetation (23%), open water (6%), golf courses (5%), and cropland, bare land, and beach (combined 1%) comprising the rest of the basin. Although the most seaward stretch of Dogwood Swash experiences tidal exchange through a concrete-lined channel, a 40 m broad-crested weir situated 200 m inland of the beach permits only offshore flow from a detention basin at the lower reaches of Dogwood Swash. Inland, the swash incises the land creating a natural bank made of soils and sediments held in place by overlying vegetation. Some parts of the lower swash basin are lined with steel

bulkheads to prevent erosion of the detention basin shoreline. This lower basin was engineered with a function similar to that of a detention pond (Schueler 2000; Drescher et al., 2007), acting as a stormwater runoff catchment and settling tank for water and materials before entering the ocean.

Inland Tributaries

Selected tributaries include T1, T2, and T3 (north to south) respectively located 1.3, 2.1, and 2.5 km inland of the time-series deployment near the mouth of Dogwood Swash (see Fig. 1). The T1 basin encompasses an area of ~1 km^2 influenced primarily by developed lands (60%) and golf courses (20%). T2 drains 0.09 km^2 influenced entirely by development (95%) and upland forest (5%). Lastly, the T3 drainage basin (~1.5 km^2) is uniquely influenced by nearly the same degree of developed and undeveloped land (48% and 42%, respectively).

Research Approach

Our approach to constructing water budgets for Dogwood Swash defines discharge over the weir as the only system output, and accounts for surface runoff, groundwater, and direct precipitation as the input sources. While we define a single output term, our approach allows additional fluid losses (e.g., evapotranspiration) from the system without compromising our estimated source water fractions. That is, the rate and magnitude of combined source inputs is not forced equal to the output rate (discharge), as we compute total discharge from Dogwood Swash and then independently resolve each source component. So, source water fractions are determined independent of extraneous factors (e.g., swash discharge and volume). Source-specific discharge rates are then calculated using temporally overlapping fraction and total discharge values. Time-series water budgets are determined for fluid fractions as well as

discharge rates, comprised of many individual water budgets, each representing the relative magnitude of fluid sources over a discrete time.

Total Discharge

The volume of water flowing over a flow control structure at any instance may be mathematically expressed as:

$$Q = \left(\frac{8}{27} g\right)^{\frac{1}{2}} * h_{weir}{}^{\frac{3}{2}} * w_c \qquad (1)$$

(Hornberger et al., 1998**)** where volumetric discharge (Q) is given by the gravitational constant (g), the difference in elevation between the water surface and weir crest (h_{weir}), and the length of weir over which water is flowing (w_c). This equation is first used to determine total discharge from the swash and then to generate water budget exports. To constrain the parameters driving these calculations, we deployed a submersible CTD data logger (Solinst, LTC Levelogger Junior) 20 cm above the swash bottom to monitor swash water level (5 min. intervals) near the weir. Data were barometrically compensated using a similar probe (Solinst Barologger Gold) that remained subaerial throughout sampling. Corrected level data were converted to water surface elevations by adding each measured water level to the constant elevation of the probe determined using RTK GPS. To ensure our surface water elevations were all determined using the same datum, we deployed the CTD in a vented PVC pipe, fixed to our time-series sampling platform. The CTD was suspended from a locking cap (to prevent infiltration of direct precipitation) and rested on the bottom of the capped PVC housing. RTK GPS methods were used to determine position and elevation of the CTD and points along the weir crest. We then determined h_{weir} for all water level measurements by calculating the difference in elevation between flooded weir sections and that of the water surface on 5 minute intervals. Here, a flooded weir section is considered to be a section of weir at lower elevation than that of the water

surface in the lower swash basin. Because a 16 cm range in elevation exists along this weir crest (in discrete segments of uneven lengths), we determined the length of each flooded weir section and summed those of equal elevation to give a single w_c value for a given swash surface elevation. Equation 1 was solved for each possible value of w_c (1 cm increments of h_{weir}) to derive an empirical discharge value for each possible value of h_{weir} and total discharge is given by the summation along the length (w_c) of flooded weir crest. To verify these discharge estimates, we measured discharge rates ~10 m downstream of the weir at low tide using a handheld Acoustic Doppler Velocimeter (ADV) FlowTracker (Sontek/YSI Inc.).

Groundwater Fraction

Relative to surface and meteoric waters, groundwaters are enriched in ^{222}Rn through interaction with uranium rich sediments, making radon an ideal tracer of groundwater inputs to surface waters (Burnett et al., 2006; Swarzenski, 2007; Charette et al., 2008). Well established methods and instrumentation exist for converting measured radon activities to quantitative groundwater estimates after a few corrections are applied (Cable et al., 1996; Corbett et al., 1999; Burnett et al., 2001). To estimate the role of groundwater in the Dogwood Swash water budget, we used a mass balance approach based upon Burnett and Dulaiova (2003) to correct the measured ^{222}Rn concentration for losses (decay and atmospheric degassing) and additional inputs (ingrowth from dissolved ^{226}Ra parent) for each measurement interval. Each corrected radon concentration can then be used to calculate a fraction of groundwater in a water body and per unit volume of discharging water following methods by Peterson et al. (2010), thus resolving the groundwater fraction and corresponding discharge value for each measurement interval. A conceptual schematic as well as a detailed description of groundwater fraction and discharge derivations used here is offered in the seminal work by Peterson et al. (2010), from which this

work is based. While some of the equations and assumptions used to generate groundwater estimates are stated throughout the coming sections, a more detailed description (including a *sensitivity analysis*) can be found in Peterson et al. (2010). Further concepts related to data presented here are discussed on pages 27 through 29 in this work in the section titled *Groundwater Model Sensitivities.*

Our ability to detect elevated radon concentrations in swash surface water suggests groundwater has discharged into the swash, but does not reveal the input location (and therefore residence time of any particular radon atom, which is an important factor to constrain the degree of decay and degassing). To address this potential complication, we used an approach by Peterson et al. (2010) that brackets the likely range of groundwater concentrations and discharge fluxes from a surface water body. Minimum calculations assume all ^{222}Rn was input proximal to the monitoring location and therefore the measured concentration equals the initial concentration as no losses would occur during the short transit. Maximum calculations assume all ^{222}Rn was input at the upstream extent of our sampling domain and is therefore subject to decay and degassing losses during the entire downstream transit, so the measured concentration is less than the initial concentration and must be corrected. Minimum groundwater discharge estimates were generated using the following equation:

$$Q_{GW}\left(\frac{m^3}{s}\right) = \left[\frac{Rn\ Conc.\left(\frac{dpm}{m^3}\right) - Bkgd.\left(\frac{dpm}{m^3}\right)}{End-member\left(\frac{dpm}{m^3}\right)}\right] Q_{TOTAL}\left(\frac{m^3}{s}\right) \qquad (2)$$

(Peterson et al., 2010) where Q_{GW} is the calculated groundwater discharge, $Rn\ Conc.$ is the measured ^{222}Rn activity for a given interval, $Bkgd.$ is supported ^{222}Rn via decay of ^{226}Ra, $End-member$ is the corresponding ^{222}Rn groundwater concentration (as measured from the aquifer), and Q_{TOTAL} is total swash discharge. This equation essentially calculates the fraction of swash water that is derived from groundwater (as excess surface activity divided by groundwater

activity) and multiplies the fraction by total discharge to derive the groundwater-borne discharge rate from the swash.

Maximum groundwater discharge estimates were then determined by:

$$Q_{GW}\left(\frac{m^3}{s}\right) = \left[\frac{\left[Rn\ Conc.\left(\frac{dpm}{m^3}\right) + \left[\frac{Atm.Evas.\left(\frac{dpm}{m^2 sec.}\right)R(sec.)}{Depth\ (m)}\right] - Bkgd.\left(\frac{dpm}{m^3}\right)\right]e^{\lambda R}}{End-member\left(\frac{dpm}{m^3}\right)}\right] Q_{TOTAL}\left(\frac{m^3}{s}\right) \qquad (3)$$

(Peterson et al., 2010). Here, each measured radon concentration ($Rn\ Conc.$) is assumed to be that which remains of the initial concentration after loss to atmospheric evasion ($Atm.Evas.$) and decay ($e^{\lambda R}$) in transit to our monitoring site. Where the magnitude of loss to the atmosphere is dependent upon the concentration gradient and turbulence associated with the air/water interface (Burnett and Dulaiova, 2003) and influenced by water depth ($Depth$). Data used to assess turbulence at the interface including air temperature and wind speed were downloaded from a public meteorological database representative of local conditions (www.ysieconet.com) and evasional losses were calculated according to MacIntyre et al. (1995). Radon lost to decay ($e^{\lambda R}$) was determined using the decay constant of ^{222}Rn (λ) ($1.56*10^4$ sec.$^{-1}$) and transit time (R) of a given concentration (see Peterson et al., 2010 for a detailed description of Eq.'s (2) and (3)). Our maximum calculations determined total loss (atmospheric evasion and decay) using the mean life of ^{222}Rn (4.79×10^5 sec.) as a constant residence time given the half-life of the isotope and the probability of detection (see *Groundwater Model sensitivities*, page 28). After correcting each measured activity for losses, we account for supported ^{222}Rn ($Bkgd.$) and divide the resultant by the ^{222}Rn concentration in the groundwater ($End-member$). Because our maximum estimates assume all radon was input upstream, we used the mean $Bkgd.$ and $End-member$ values representative of the three

upstream tributaries rather than those values measured at the downstream site (see *Groundwater Model Sensitivities*, page 28 for a detailed discussion regarding end-member constrainment). As this approach constrains the range of possible groundwater discharge fluxes (Peterson et al., 2010), groundwater discharge estimates are presented here as a mean of our minimum and maximum estimates.

To construct a long-term record of ^{222}Rn concentrations, we deployed an automated radon system as described by Burnett and Dulaiova (2003) fixed to a stationary platform situated ~5 m from the northern swash bank. In short, a submersible pump (secured ~20 cm above the swash bottom) delivered surface water to a degassing chamber (RAD-Aqua; Durridge Co.) where air-water equilibration of radon-222 was achieved. Air from the chamber was then pumped through desiccant to a radon-in-air monitor (RAD7; Durridge Co.) where gaseous radon activities were measured via alpha counting. To correct each measurement for additional ^{222}Rn sources, we subtracted the ^{222}Rn produced from decay of the suspended parent isotope (^{226}Ra) from the total activity to yield excess ^{222}Rn. Ra-226 activities were measured by collecting and filtering large volumes (~62 L) of swash water through MnO_2-impregnated acrylic fibers that quantitatively adsorb radium (Moore and Reid, 1973), and measured the fibers for ^{226}Ra using methods outlined by Peterson et al. (2009).

To constrain groundwater end-member ^{222}Rn activities, we sampled groundwater directly from piezometers constructed using 1 in diameter PVC pipe with 10 cm screened sections installed 1.5 m, 1.25 m, 1.0 m, and 0.5 m below ground surface in the adjacent aquifer. Groundwater was collected in 250 mL glass bottles (WAT-250 system; Durridge Co.) using a peristaltic pump and measured using standard RAD7 protocols. In addition to direct groundwater sampling, we used a laboratory incubation method to constrain end-member activities using

aquifer materials from depths consistent with each piezometer. By this method, 100 g of dry sediment was sealed in a 300 mL Erlenmeyer flask with radium-free water for 21 days to achieve secular equilibrium between ^{222}Rn and sedimentary ^{226}Ra **(**Corbett et al., 1998). After 3 weeks, samples were measured using similar instrumentation and procedures as for groundwater field samples. Because groundwater becomes enriched in ^{222}Rn through decay of the parent isotope, the ^{222}Rn concentration in the overlying water represents that which would be generated in groundwater with at least a three week residence time within the aquifer, a maximum estimate of groundwater ^{222}Rn activities.

While our ^{222}Rn time-series deployment was active, we collected surface water in 7 L Nalgene bottles (Stringer and Burnett, 2004) each week. Samples were analyzed for ^{222}Rn according to Lee and Kim (2006) while supported and end-member ^{222}Rn activities were determined for each tributary following identical sampling techniques and analyses as previously described. Water budgets for each tributary are used to primarily assess the relatedness between source water dynamics and budget stability through time to impervious cover in an effort to place downstream results in larger context.

Direct Precipitation Fraction

To resolve the contribution of direct precipitation (falling onto the open water portions of Dogwood Swash) to the total water budget, we compared the volume of precipitation (average over a given interval) to that of the swash over the same period. Local precipitation accumulation was measured using an automated ISCO sampler and accompanying rain gauge located ~50 m east of the ^{222}Rn time-series deployment. We then digitized an aerial image of the basin to determine the surface area of the swash subject to direct precipitation and multiplied the accumulated rainfall by the surface area of the swash to generate volumetric precipitation inputs.

To determine the volume of the swash at a given instance, we conducted a bathymetric survey using single-beam sonar methods and RTK GPS where position and depth data were digitally recorded and processed using hydrographic survey software (Hypack Inc.). Briefly, survey data were collected using a canoe outfitted with a GPS antenna and single beam sonar transducer fixed just below the water surface. For depths too shallow to be surveyed by this method, we traversed the area of interest with a GPS antenna mounted pack. Discrete elevations of the swash bottom were imported to GIS where a bathymetric surface was created and bound by the area of open water determined using aerial imagery. Swash volume estimates were generated using GIS (3D Analyst: Functional Surface) as the three dimensional volume between the bathymetric surface and the water surface. To apply this approach through time, we used our time-series elevation-corrected depth record to generate a representative range of surface water elevations that would serve as the vertical bounding surface for which our calculations considered. After several computations (n=16) using surface water elevations ranging from 1.78 m to 2 m, we used liner regression to generate empirically derived predictions of total volume as a function of water depth. To determine the fraction of precipitation within the swash, we simply divide the average volume of direct precipitation by that of the swash. Direct precipitation discharge is then determined by multiplying the fraction of direct precipitation by total swash discharge. Tributary water budgets are comprised only of groundwater and surface runoff (overland flow + direct precipitation) as the open water area for each tributary is negligible in comparison to that of Dogwood Swash.

Surface Runoff Fraction

Surface runoff is defined here as, the precipitation that falls on the terrestrial drainage basin and is subsequently conveyed to Dogwood Swash through engineered drainage networks

(pipes and ditches) as well as sheetflow runoff. Combined surface runoff, groundwater, and direct precipitation inputs comprise the total budget at any instant. To resolve surface runoff contributions, we subtract groundwater and direct precipitation fractions from the total budget (100%) to yield the swash surface runoff component. Resulting fractions of surface runoff are then multiplied by total swash discharge rates to determine surface runoff export rates.

Results and Discussion

Dogwood Swash water budgets are presented for both *fractions* of swash fluid (%; surface runoff, groundwater inputs, and direct precipitation) and *discharge rates* (m^3/s; total, surface runoff, groundwater, and direct precipitation) from September 1, 2011 through October 8, 2013. We present these water budgets as both *high-resolution* (at 30 minute intervals) and *monthly mean* values for a more comprehensive assessment of temporal variability. By our convention, direct precipitation fractions are negligible (0, except during times of rainfall) in our high-resolution records and therefore these results are not shown on this time scale. However, over much longer time scales (e.g., months to years), direct precipitation to the swash water surface represents a measurable fraction of the budget, and is therefore included in the monthly mean results. So, our high-resolution water budgets include two terms: surface runoff and groundwater, while our long-term budgets are comprised of three terms: surface runoff, groundwater, and direct precipitation.

The absolute volume of Dogwood Swash, at any instant, is a combination of source waters, where total volume equals the summation of fluid contributions from each source. In constructing these water budgets, we examine the role of each source within the swash and how each relates to the relative magnitudes of export from the system. Field observations of ^{222}Rn activities varied considerably (from 0.13 dpm/L ± 0.09 dpm/L to 22.75 dpm/L ± 1.24 dpm/L) with an average activity of 6.19 dpm/L (± 0.65 dpm/L) (Fig. 2A). Measured activities were then converted to minimum and maximum groundwater percent fractions (Eq. 2 and Eq. 3, respectively) where average minimum groundwater fractions were 4.22% (ranging from 0.02% to 15.98%) and average maximum groundwater fractions were 6.38% (ranging from 0.23% to 65.26%) (Fig. 2B). As applying Eq. 2 and Eq. 3 generates similar groundwater fraction

estimates, we apply an average of the two results to our water budgets yielding a single groundwater fraction estimate for each 30 min. interval. From this, we determined surface runoff generally constitutes a substantial component of the total budget while groundwater fractions are much less (Fig. 3A). On average, Dogwood Swash is comprised of 94.4% (ranging from 63.52% to 99.97%) surface runoff, 5.6% (ranging from 0.03% to 36.48%) groundwater, and 3.2×10^{-3}% (ranging from 0.0% to 7.7×10^{-3}%) direct precipitation. Because the swash was engineered primarily to act as a stormwater-runoff catchment, it is logical that surface runoff constitutes 16.8 times more volume than groundwater, and nearly 30,000 times that of direct precipitation. While these values represent a broad evaluation of the swash water budget, we will examine temporal variability of the system in the following sections.

Our water budgets represent the nature of the fluids within the swash and discharging real-time from the swash at the outlet, so do not necessarily reflect when these waters entered the swash body. Interpretations of Dogwood Swash water budgets consider two perspectives: the first focused strictly on the swash as an isolated system primarily using fluid fractions and their relative contribution to the total budget (as above); the second perspective emphasizes the intimacy between the swash and the nearshore water it drains into, highlighting the importance of the swash as a point-source for water and associated constituents (e.g., nutrients, metals, and bacteria) to a larger coastal ecosystem. Discharge rates from the swash thus represent the influence of Dogwood Swash as a contributor of fluid and materials to Long Bay. In general, discharge from the swash was quite variable from 2011 through 2013 (Fig. 2C). The average rate of discharge from the swash was 0.030 m^3/s with a standard deviation of 0.027 m^3/s, ranging from 0.00 m^3/s to 0.553 m^3/s. For comparison, Little River, located ~46 km NE of Dogwood Swash, discharged at an average rate of 16.12 m^3/s into Long Bay over the same interval

(www.dnr.sc.gov). While the average discharge rate from Dogwood Swash represents a small fraction of that from Little River, applying this rate to each of the fifteen swashes in the Grand Strand totals 35.5% of the average discharge rate from Little River, a major inlet along the Grand Strand.

Temporal Trends

Long-term

Understanding how the Dogwood Swash water budget functioned during our study is an important first step, but an examination of how the budget behaves over various time scales allows a more comprehensive assessment of how this swash (and similar water bodies in urban drainage basins) respond to external driving forces (e.g., weather, climate, and development intensity). To analyze yearly change, we compute monthly average source-specific fraction and discharge rates (Table 1) for months containing sufficient data to calculate water budgets for at least 70% of the month. This equates to roughly three weeks of water budget results each month, which we consider adequate to represent the monthly conditions. To compare 2012 to 2013, only those months that meet these criteria in both years of the study are averaged (Table 2). Thus, we consider January through June in our yearly interpretations as these were the only overlapping records between 2012 and 2013. While the yearly average values presented in Table 2 are useful for annual comparisons, they do not represent the entire annual conditions of the Dogwood Swash water budget.

Our two year time-series water budgets indicate an overall change in Dogwood Swash fraction dynamics between 2012 and 2013 (Fig. 3A). We observed an increase of 2.7% in surface runoff fraction from 2012 (92.3%) to 2013 (95.1%; Table 2). Likewise, groundwater fraction decreased by 2.7% over this same time frame (from 7.7% in 2012 to 4.9% in 2013; Table 2). To

examine change in swash fraction, we computed source water ratios (SWR) by dividing the percentage of surface water within the swash at any instant by that of groundwater. Theoretically, the SWR ranges from zero approaching infinity, where a value of zero represents a system comprised entirely of groundwater and approaches infinity as surface water fraction increases toward 100%. It is worth mentioning that the same SWR value can be derived using either fraction or discharge values, however each has an operational threshold. Computations using fraction or discharge can result in errors when groundwater fractions equal zero, while similar errors result when using discharge values during times of no flow. For this reason, calculations are based on fraction results as some fraction of groundwater always existed in the swash during our study period. In doing so, we see average annual SWR increases by 63% (from 24.2 to 47.5) indicating a substantial change in source waters to Dogwood Swash (Figure 3A).

Over this same interval, average precipitation rates increased (Figure 3B) as well as the fraction of direct precipitation within the swash (Table 2). Although the precipitation component of the total budget is inherently dependent upon total swash volume (by the nature of our calculations), average precipitation rates increased in 2013 (from 0.086 mm/hr to 0.116 mm/hr; January through June) while the volume of the lake remained nearly constant (a change of 0.02%), suggesting the increase in direct precipitation fraction (from 2.7×10^{-3} % in 2012 to 3.6×10^{-3} % in 2013) largely reflects the increase in rainfall, rather than a change in volume of the swash.

Total discharge rates increased by 26% from 0.029 m^3/s to 0.036 m^3/s from 2012 to 2013 (Table 2). Although total discharge was lower in 2012, more intense discharge pulses were observed during this year (reaching 0.56 m^3/s) compared to 2013 (up to 0.32 m^3/s) (Figure 3C). While direct precipitation to the swash surface comprises a negligible component of the water

budget (always less than 0.008% of the budget), the increase in total discharge from Dogwood Swash in 2013 is likely attributed to the increased rainfall and subsequent runoff from the drainage basin as additional factors (e.g., elevation of the weir) remained constant.

Consequently, long-term trends in total discharge rates and source waters observed at Dogwood Swash result in source-specific discharge rate changes. Considering the increased discharge rate, and the increased surface runoff fraction, a 30% increase in surface runoff discharge was observed from 2.7×10^{-2} m^3/s to 3.4×10^{-2} m^3/s although swash surface runoff fractions within the swash only increased by 3%. Despite increases in total discharge rates, decreases in groundwater fraction (by 35%) lead to an accompanying 14% decrease in groundwater flux out of the swash (from 2.4×10^{-3} m^3/s to 2.0×10^{-3} m^3/s; Table 2). These results suggest an increase in surface drainage efficiency (i.e., less infiltration to groundwater) under increased precipitation rates.

To further understand the fractional decline of groundwater in Dogwood Swash, we examine ^{222}Rn activities in the adjacent aquifer to estimate groundwater residence times (Fig. 4). To calculate residence times, we use our laboratory incubation ^{222}Rn end-member (414.2 dpm/L) and those measured in the field (minimum 73.7 dpm/L; maximum 253.5 dpm/L). Incubation results represent equilibrium between parent (^{226}Ra, enriched in sediments) and daughter (^{222}Rn) isotopes, a process that takes approximately three weeks. Radon activity in groundwater samples increases as a function of residence time in the aquifer, generating a reproducible in-growth curve where we then solve for residence time at a given activity. In doing so, we see a significant increase in groundwater residence times within the aquifer, from 1.8 to 3.2 days (r^2=0.259, n=16, α=0.05) through our study, indicating a decrease in groundwater velocity and subsequent rate of discharge to the swash.

Seasonal

To examine seasonal variability in fluid fractions and discharge rates from Dogwood Swash, we averaged monthly water budget parameters to generate seasonal groups considering both 2012 and 2013 (Fig. 5). We define winter as December through February, spring as March through May, summer as June through August, and fall as September through November. In total, we sampled seven seasons including two winters, springs, and summers while capturing only fall of 2012. In general, seasonal trends were evident in Dogwood Swash fractions with inverse correlations between surface runoff and groundwater fractions. On average, surface runoff fractions were lowest during spring months when groundwater fractions were highest (92.7% and 7.3%, respectively; Fig. 5A). Conversely in fall, surface runoff fractions were highest (96.3%) when groundwater fractions were lowest (3.8%). Direct precipitation fractions follow average seasonal rainfall rate trends with summer being the highest for both (4.5×10^{-3}%; 0.142 mm/hr) and lowest in fall (2.0×10^{-3}%; 0.064 mm/hr). With the exception of summer months, precipitation fractions negatively correlate with surface runoff and positively correlate with groundwater fractions within the swash (Fig. 5A).

Considering precipitation to be the primary recharge mechanism for the shallow aquifer, it seems reasonable that groundwater fractions in the swash generally trend with precipitation rates. However, in summer, average precipitation rates were 30% higher than spring, yet groundwater fractions were generally quite low. Data from long-term water table monitoring efforts in Briarcliffe Acres (approximately 28 km NE of the swash outlet) show prominent seasonal trends in water table height with maximum elevations in summer (Libes and Peterson, 2014). Researchers (e.g., Xue and Gavin, 2008; Cerda, 1997) have shown rainwater infiltration efficiencies (and groundwater production rates) decrease with higher soil moisture content (here,

a likely result of increased precipitation and water table height) as porous aquifer material becomes saturated. In this case, high regional water tables in summer inhibit infiltration of the abundant precipitation, converting a greater portion to surface runoff. Subsequently, summer surface runoff fractions rivaled the highest measured, while the fraction of groundwater in the swash was 25% lower than the long-term average, despite high rainfall rates. Likewise, in spring and winter months, when infiltration efficiencies are higher (and precipitation rates are lower), surface runoff fractions decrease while groundwater fractions increase. We exclude fall months in these interpretations as we only sampled through fall of 2012 and long-term trends suggest significant change in 2013.

Much like seasonal changes in Dogwood Swash fractions, we observed changes in discharge rates from the swash on seasonal scales (Fig. 5B). Average total discharge from the swash was highest in the spring (0.0384 m^3/s) followed by winter, summer, and fall (0.0211 m^3/s). We suspect evaporative losses from the swash to be highest in summer as discharge rates are decreased during this time despite high rainfall rates. Work by Grimmond and Oke (1986) and Hanrahan et al. (2010) emphasize the importance of seasonality in evaporation losses representing a significant removal mechanism from surface water bodies during summer months. Governed by increased total discharge, spring months generated the highest average source-specific output rates from the swash for all parameters (surface runoff 0.0355 m^3/s; groundwater 2.9×10^{-3} m^3/s; direct precipitation 1.4×10^{-6} m^3/s) (Fig. 5B). Although surface runoff fractions within the swash are lowest during the spring, increases in the total system output deliver more surface runoff in spring than any other season (23% more than winter; 46% more than summer; 74% more than fall). Groundwater fractions in the swash positively correlate with the magnitude

of groundwater discharged from the swash throughout all seasons (spring 2.9 x 10^{-3} m^3/s; winter 1.8 x 10^{-3} m^3/s; summer 1.2 x 10^{-3} m^3/s; fall 7.8 x 10^{-4} m^3/s) (Fig. 5).

Not only did we observe seasonal trends in Dogwood Swash water budgets, but also in the *timing* of the seasons. In general, the highest rainfall rates occur during spring and summer seasons in eastern South Carolina when we see direct precipitation fraction maxima in Dogwood Swash (Fig. 6A). However, monthly mean precipitation rates and direct precipitation fractions peak earlier in 2013 than in 2012 (Fig. 3B; Table 1). In 2012, average spring precipitation rates peak in May (0.202 mm/hr) and the summer peak occurs in August (0.194 mm/hr), whereas the average 2013 peaks appear in April (0.244 mm/hr) and June (0.202 mm/hr). Subsequently, we see spring surface runoff fraction minima occur earlier in 2013 than 2012 (May 91.6%; April 92.5%) and similar shifts in groundwater fraction maxima (May 2012 8.4%; April 7.5%) (Table 1). Furthermore, total and source-specific outputs from the swash peak earlier in 2013 than 2012 altering the schedule of maximum fluid and material delivery to the nearshore (Fig. 6B). These timing shifts are not unique to the Dogwood Swash system; peak water table elevations at Briarcliffe Acres occur on August 31 in 2012 and shift to July 31 in 2013 (Libes and Peterson, 2014), providing regional scale evidence of temporal seasonal shifts.

Short-term Events

The long-term water budget dynamics represent the interplay between runoff inputs from surficial and subsurface pathways and discharge patterns integrated over many rain events. Here, we examine specific, short-term events following both dry and rainy periods to put the long-term trends into context. During a six day period of rain-free conditions (September 28-October 3, 2013) following a relatively dry period, swash system dynamics reflect a stable system (Fig. 7). On average, swash levels fluctuate 1.5 cm/day (ranging from 0.688 m to 0.710 m), while

groundwater levels fluctuate 2.7 cm/day (1.05 m to 1.08 m) (Fig. 7A). Both swash and groundwater levels peak in early morning (02:00-07:00) with lows in the evening (15:00-18:00), a likely result of evapotranspiration following diel photosynthetic patterns (Lautz, 2007; Winter, 1999). Evapotranspiration-driven changes in water levels (swash and groundwater) alter swash fractions (water level is inversely related to the SWR) and discharge rates from the swash (positive relationship with discharge rates) (Fig. 7). As a result, discharge pulses negatively correlate with the SWR, exporting lower fractional ratios of surface runoff to groundwater in high discharge pulses during dry periods (Fig. 7B).

For comparison, we examine eight days (June 2-June 9, 2013) of water level, fraction, and discharge data during several days of rainfall (Fig. 8). During this time, rainfall amounts totaled 90.7 mm and primarily occurred during three days (June 3rd, 6th, and 7th) following dry antecedent conditions (date of last rainfall: May 23rd). Those depicted in Fig. 8A are examined as three separate events; the first totaled 25.7 mm, the second totaled 10.9 mm, and the third totaled 54.1 mm. Swash water levels and water table heights both respond within an hour of rainfall onset, however, groundwater levels require substantially more time to stabilize after the conclusion of the rain event due to the nature of flow through a porous matrix in the aquifer (Fig. 8A). Following each event, the SWR increases indicating fractional shifts toward higher surface-runoff dominance (Fig. 8B). Since surface runoff pathways convey water to the swash much more quickly than subsurface pathways, the post-event SWR decreases through time (indicating less surface runoff and more groundwater) as the aquifer drains and elevated groundwater levels stabilize. With the exception of the second event, swash levels stabilize approximately 1.5 hours post-event (albeit at a higher level) after the first flush of rainfall pulses swash water out of the system. The decrease in swash level and total discharge rates following the second rain event are

a result of a shift in wind direction from SW to SE (www.ysi.econet.com). Because the long-axis of Dogwood Swash is oriented NW to SE, a SE wind forces water away from our monitoring station and the weir resulting in discharge decreases. At the onset of the third precipitation event, the prevailing SW wind returns, dramatically increasing discharge rates (from 3.7×10^{-4} m^3/s to 0.190 m^3/s) and swash levels (from 0.67 m to 0.74 m).

While the response time of the swash and aquifer remained fairly constant throughout the three events, the magnitude and timing of these fractional shifts are unique to each event. Following the first event, the SWR increased to 287.5 (the average pre-event SWR was 57.6) 13 hours after the event, indicative of increased surface runoff fractions within the swash (Fig. 8B). This result is somewhat expected: a pulse of surface runoff immediately following the rainfall increases the SWR, is then quickly conveyed out of the system after which time diffuse groundwater inputs begin to dominate, reducing the SWR below normal levels. Despite a lower rainfall total than the third event, we observed the highest surface runoff fractions (as per the SWR) in the swash following the first event (Fig. 8B). The maximum SWR following the second event was much lower than the first (52.4) and occurred 3.5 hours earlier. The low value of this peak suggests the swash contained a greater fraction of groundwater (a result of continued aquifer discharge from the first event) than before this rain event began (Fig. 8B). The earlier occurrence of the maximum SWR is likely a result of the timing of the third event (beginning only 13 hours later). Nearly two days after the third event, the SWR peaks at 260.5. Prior to this, maximum water table height exceeds those of the other events (10 cm and 14 cm greater than water table levels associated with the first and second event, respectively) in response to increases in precipitation amounts. The increase in water table height subsequently increases the amount of time necessary to stabilize levels. As a result, the SWR remains relatively low

following the event, as groundwater continues to seep into the swash from the saturated aquifer. When groundwater levels stabilize approximately 40 hours post-event, the SWR reaches its maximum indicating a decrease in groundwater inputs to the system. These results suggest complex interactions between surface runoff conveyance efficiency and drivers of groundwater to the swash, related to the conditions during and preceding rain events.

We assess drainage basin conveyance efficiency for each precipitation event by comparing the volume of water output from the swash to the volume of rain that fell on the impervious portions of the basin over the same interval. During the June 2013 events, an average of 24.1% of the equivalent rainwater volume delivered to the impervious areas of the basin was discharged within 12 hours after the event (event 1: 19.1%, event 2: 31.0%; event 3: 22.3%), and more than half (58.3%) was discharged from the swash within two days. Fitting this percentage over various periods of time, a linear equation suggests that a volume of water equal to that which fell on the area of impervious cover within the Dogwood Swash basin will be discharged from the swash in 3.5 days ($y=1.2068x$; where percent volume discharged (y) is a function of time (x); $r^2=0.85$, $n=5$, $\alpha=0.05$). Though we assess isolated rainfall periods here, these results are indicative of perturbations to the relatively stable swash system when no rainfall occurs, and extrapolate to the longer-term periods described above.

Basin Development

We evaluate the relationship between the degree of impervious cover within the urbanized Dogwood Swash basin and contributing sources to the water budget by examining three upstream tributaries and their respective watersheds, each a sub-basin within the larger Dogwood Swash drainage complex. In total, 85 weeks (from September 2011 to September 2013) of fraction data were recorded for each site (T1, T2, and T3; Fig. 9). On average, T1 was

comprised of 85.0% surface runoff and 15.0% groundwater, T2 was comprised of 95.3% surface runoff and 4.7% groundwater, and T3 was comprised of 84.1% surface runoff and 15.9% groundwater. The fraction of surface runoff within each tributary is positively correlated with the degree of impervious cover within the basin, and inversely related to groundwater fraction and temporal fraction variability (Fig. 9). The T3 water body drains the least urbanized basin (48% impervious) and was comprised of relatively low surface runoff fractions and high temporal source water variability (standard deviation= 19.2) (Fig. 9A). The T1 basin is characterized by medium development (60% impervious) with higher average surface runoff fractions and less temporal change in source water records (standard deviation=9.2) (Fig. 9B). T2, the most developed basin (95% impervious) had the highest average surface runoff fraction and the least variability through time (standard deviation=2.3) (Fig. 9C).

Despite sampling through numerous rain events, drought periods, and seasonal fluctuations, a robust relationship exists between impervious drainage area and fluid fractions for these tributaries. It is well documented that urbanization alters hydrologic processes (e.g., Grimm et al., 2008; Hasse 2009) by increasing surface runoff and decreasing groundwater recharge associated with rainfall (Corbett, C.W. et al., 1997; Loucaides et al., 2007; Raffernsperger and Cochrane, 2010). We calculate aquifer residence times for the sub-basins to examine how development-driven decreases in aquifer recharge relate to decreased groundwater fractions in the urban streams of the Dogwood Swash basin. The average residence time of groundwater entering the T3 tributary, transiting through the least impervious basin, was less than half that of T1 groundwater, influenced by more impervious surface area (2.7 days and 6.5 days, respectively). Analyses of aquifer material porosity and grain-size between each tributary indicate subsurface homogeneity between study sites in the Dogwood Swash drainage basin

suggesting the residence time differences are related to impervious surface area. While a fraction of rainwater may percolate through impervious surfaces to recharge the urban aquifer (Ragab et al., 2003), these results suggest groundwater transport rates in highly urbanized areas are less than those associated with lower degrees of impervious cover. Our data indicate that altering rainwater infiltration areas and rerouting subsurface flowpaths in highly urban areas increases groundwater residence times, thus reducing inputs to receiving waters.

Urbanization-related changes in timing and magnitude of source-water delivery to coastal streams and nearshore waters can significantly impact the physiology of these systems. A review by Paul and Meyer (2001) shows the majority of urban streams receive high nutrient loads and exhibit greatly reduced nutrient removal efficiencies, increasing nutrient loads to downstream waters. Locally, Hutchins et al. (2014) documented DOC and organic nutrient enrichments in urban surface runoff relative to urban and pristine groundwaters. Furthermore, additions of urban surface runoff to coastal ocean waters stimulated the largest phytoplankton and bacterioplankton production responses than nearby groundwaters (Hutchins et al., 2014). These results suggest further increasing surface runoff inputs to Dogwood Swash and other similar catchments could result in higher nutrient loading to the system and subsequently the nearshore receiving waters.

Groundwater Model Sensitivities

Our water budget approach delineates groundwater fraction from the total swash budget using a geochemical tracer approach (^{222}Rn; Peterson et al., 2010) and direct precipitation fraction via volume ratios, whereas surface runoff is resolved by difference. As direct precipitation constitutes a small fraction of the budget, groundwater fraction estimates direct our surface runoff fraction and discharge estimates. Uncertainties inherent to these calculations include ^{222}Rn end-member constrainment (Eq. 2, Eq. 3) and transit times (Eq. 3) of upstream

waters to our downstream monitoring location. While additional ^{222}Rn may be contributed to the system via diffusive fluxes from bottom sediments (e.g., Corbett, R.C. et al., 1998), previous studies indicate that these contributions are often minimal in advective systems (Lambert and Burnett, 2003; Gleeson et al., 2013). In fact, calculations suggest average diffusive ^{222}Rn fluxes (5.91 dpm/m^2/0.5 hr) contribute negligible concentrations (4.34 dpm/m^3) to the average of those observed in the swash (6192.4 dpm/m^3) and are not considered in our water budget calculations.

The most common source of uncertainty in ^{222}Rn tracer studies lies in end-member selection (Corbett et al., 1997; McCoy et al., 2007; Santos et al., 2009; Dimova and Burnett, 2011) as groundwater ^{222}Rn activities can vary significantly in space and time (Mullinger at al., 2009; Dulaiova et al., 2008). To best estimate representative end-members in our system, we conducted sixteen end-member sampling campaigns at our downstream monitoring site and inland tributaries (T1, T2, and T3) from September 2011 through September 2013, sampling through wet and dry conditions throughout all seasons of both years. Dulaiova et al. (2008) suggest end-member selection considers porewater chemistry heterogeneity with depth and variable sediment surface chemistry as well as seasonal fraction variations in discharged groundwaters. In an effort to best constrain representative end-members for our water budget calculations, we collected vertical end-member profiles (n=4) at most sites and use an average to represent our groundwater end-member. The nearest sampled end-member in space and time was then applied for each 30-minute interval of our groundwater model (Eq. 2 and Eq. 3). Peterson et al. (2010 discuss quantitative impacts of end-member variability in this groundwater model.

The transit time of upstream waters to the downstream monitoring site governs the length of time over which corrections are made for atmospheric evasion and decay losses in our maximum groundwater fraction estimates (Eq. 3). As a conservative estimate of Dogwood

Swash basin fluid transit times, we select the mean life of ^{222}Rn (5.5 days), representing the average time a batch of radon atoms is likely to survive in the system for detection at our downstream monitoring site. In using a constant residence time, we do not assume a fixed input location of groundwaters input upstream, but rather guide our maximum estimates using a statistical measure of high detection probability after injection into the system without constraining a discrete location. It is important to then mention the residence time applied in these calculations in not one of the swash reservoir, but that of our radiotracer. To minimize the emphasis placed on this parameter, we present our groundwater estimates as an average of minimum and maximum groundwater contributions. Because our minimum estimates require no time-sensitive corrections, presenting these values as an average stands as a conservative approach, with close agreement between average model results (± 2.16%).

Conclusions

We demonstrate the utility of natural radiotracers to effectively compile long-term, high-resolution water budgets incorporating groundwater contributions to an urban stormwater catchment in the Grand Strand area of South Carolina. We consider not only fluid fractions within the stream but also source-specific outputs from the system to the coastal ocean. By constructing time-series water budgets for Dogwood Swash, we determined surface runoff fractions averaged 94.4% of the swash budget from 2012 through 2013, with groundwater fractions averaging 5.6% and direct precipitation comprising an average 3.2×10^{-3}% of the total water budget. Although data suggest surface runoff constitutes the majority of the water budget, relative surface runoff and groundwater fractions varied considerably from 2012 through 2013 (± 36.45%). By constructing long-term budgets, we were able to resolve long-term (e.g., year to year and seasonal) and short-term (e.g., precipitation events) temporal trends for a more comprehensive assessment of fluid fractions and source-specific outputs.

From 2012 to 2013, surface runoff fractions increased by 2.7% with corresponding declines in groundwater fraction due to increased aquifer residence times, in spite of greater precipitation rates. Increased total swash discharge rates in 2013 then contributed to a 30% increase in surface runoff exports from the swash, while groundwater export rates declined by 14%. Seasonal trends were also evident in swash fractions and source-specific export magnitudes with minimum surface runoff fractions in spring and maximum fractions in fall. Although seasonal groundwater fractions were inversely related to surface runoff, highest source-specific outputs of all parameters (surface runoff, groundwater, and direct precipitation) were observed in spring.

High-resolution records indicate evapotranspiration-driven changes drive short-term source fractions and exports contributing to lower fractional ratios of surface runoff to

groundwater during high discharge pulses under relatively dry periods. Although complex factors (e.g., wind speed and direction, time since last rainfall, and water-table height prior to the event) influence the timing and magnitude of fractional shifts to a more surface runoff dominated system following rain event, we determine a volume of water equal to that which fell on the area of impervious cover in the entire basin will be discharged from the swash within 3.5 days of rainfall. Data suggest increased impervious cover within a basin dampen both long-term and short-term dynamics by reducing source water variability and decreasing groundwater contributions to urban streams by increasing aquifer residence times.

Work here illustrates the utility of ^{222}Rn as a water budget construction tool to delineate groundwater sources to urban streams, a source which is demonstrated to contribute up to 36.5% of the total fluid budget for Dogwood Swash. As shown by other researchers, this approach has applications to other aquatic environments worldwide (Cable et al., 1996; Burnett and Dulaiova 2003; Lambert and Burnett 2003; Santos et al., 2009; Peterson et al., 2010). From the construction of fluid budgets, source-specific material fluxes may be determined which may be used to guide and influence management decisions. As demonstrated by the budget complexity presented here, we recommend long-term monitoring to understand system dynamics and best design sampling efforts to monitor the effectiveness of practices implemented.

References

Arnold, J.G., Allen, P.M., 1996. Estimating hydrologic budgets for three Illinois watersheds. Journal of Hydrology 176, 57-77.

Arnold, J.G., Muttiah, R.S., Srinivasan, R., Allen, P.M. 2000. Regional estimation of base flow and groundwater recharge in the Upper Mississippi river basin. Journal of Hydrology 227, 21-40.

Barron, O.V., Barr, A.D., Donn, M.J., 2013. Effect of urbanization on the water balance of a catchment with shallow groundwater. Journal of Hydrology 485, 162-176.

Booth, D.B., Hartley, D., Jackson, R., 2002. Forest cover, impervious-surface area, and the mitigation of stormwater impacts. Journal of the American Water Resources Association, 38 (3): 835-845.

Booth, D.B., Jackson, C.R., 1997. Urbanization of aquatic systems: Degradation thresholds, stormwater detention, and the limits of mitigation. Journal of the American Water Resources Association, 55 (5): 1077-1090.

Brabec, E., Schulte, S., Richards, P.L., 2002. Impervious surfaces and water quality: A review of current literature and its implications for watershed planning. Journal of Planning Literature, 16 (4). doi: 10.1177/088541202400903563.

Burnett, W.C., Kim, G., Lane-Smith, D., 2001. A continuous monitor for assessment of ^{222}Rn in the coastal ocean. Journal of Radioanalytical and Nuclear Chemistry 249, 167-172.

Burnett, W.C., Aggarwal, P.K., Aureli, A., Bokuniewicz, H., Cable, J.E., Charette, M.A., Kontar, E., Krupa, S., Kulkarni, K.M., Loveless, A., Moore, W.S., Oberdorfer, J.A., Oliveira, J., Ozyurt, N., Povinec, P., Privitera, A.M.G., Rajar, R., Ramessur, R.T., Scholten, J., Stieglitz, T., Taniguchi, M. and Turner, J.V., 2006. Quantifying submarine groundwater discharge in the coastal zone via multiple methods. Science of the Total Environment, 367: 498-543.

Burnett, W.C., Dulaiova, H., 2003. Estimating the dynamics of groundwater input into the coastal zone via continuous radon-222 measurements. Journal of Environmental Radioactivity 69, 21-35.

Cable, J.E., Burnett, W.C., Chanton, J.P., Weatherly, G.L., 1996. Estimating groundwater discharge into the northeastern Gulf of Mexico using radon-222. Earth and Planetary Science Letters 144, 591-604.

Cerda, A., 1997. Seasonal changes of the infiltration rates in a Mediterranean scrubland on limestone. Journal of Hydrology 198, 209-225.

Charette, M.A., Moore, W.S. and Burnett, W.C., 2008. Uranium- and thorium-series nuclides as tracers of submarine groundwater discharge. In: U-Th Series Nuclides in Aquatic Systems. Elsevier, Amsterdam, pp. 155-191.

Corbett, C.W., Whal, M., Porter, D.E., Edwards, D., Moise, C., 1997. Nonpoint source runoff modeling: A comparison of a forested watershed and an urban watershed on the South Carolina coast. Journal of Experimental Marine Biology and Ecology 213, 133-149.

Corbett, R.C., Burnett, W.C., Cable, P.H., Clark, S.B., 1997. Radon tracing of groundwater input to Par Pond, Savannah River Site. Journal of Hydrology 203, 209-227.

Corbett, D.R., Burnett, W.C., Cable, P.H., Clark, S.B., 1998. A multiple approach to the determination of radon fluxes from sediments. Journal of Radioanalytical and Nuclear Chemistry 236, 247-252.

Corbett, D.R., Chanton, J., Burnett, W., Dillon, Rutkowski, C., 1999. Patterns of groundwater discharge into Florida Bay. Limnology and Oceanography 44, 1045-1055.

Dimova, N.T., Burnett, W.C., 2011. Evaluation of groundwater discharge into small lakes based on the temporal distribution of radon-222. Limnology and Oceanography, 56 (2): 486-494.

Drescher, S.R., Messersmith, M.J., Davis, B.D., Sanger, D.M., 2007. State of Knowledge: Stormwater Ponds in the Coastal Zone. South Carolina Department of Health and Environmental Control – Ocean and Coastal Resource Management.

Dulaiova, H., Gonneea, M.E., Henderson, P.B., Charette, M.A., 2008. Geochemical and physical sources of radon variation in a subterranean estuary- implications for groundwater radon activities in submarine groundwater discharge studies. Marine Chemistry 110, 120-127.

Gimm, N.B., Faeth, S.H., Golubiewski, N.E., Redman, C.L., Wu, J., Bai, X., Briggs, J.M., 2008. Global change and the ecology of cities. Science 319, 756-760.

Gleeson, J., Santos, I.R., Maher, D.T., Golsby-Smith, L., 2013. Groundwater-surface water exchange in a mangrove tidal creek: Evidence from natural geochemical tracers and implications for nutrient budgets. Marine Chemistry 156, 27-37.

Grimmond, C.S.B., Oke, T.R., 1986. Urban Water-balance 2. Results from a suburb of Vancouver, British Columbia. Water Resources Research 22, 1404-1412.

Haase, D. 2009. Effects of urbanization on the water balance – A long-term trajectory. Environmental Impact Assessment Review 29, 211-219.

Hancock, P.J., Boulton, A.J., Humphreys, W.F., 2005. Aquifers and hyporheic zones: Towards an ecological understanding of groundwater. Hydrogeology Journal 13, 98-111.

Hanrahan, J.L., Kravtsov, S.V., Roebber, P.J., 2010. Connecting past and present climate variability to the water levels of Lakes Michigan and Huron. Geophysical Research Letters 37. doi:10.1029/2009GL041707.

Hildebrandt, A., Guillamón, M., Lacorte, S., Tauler, R., Barceló, D., 2008. Impact of pesticides used in agriculture and vineyards to surface and groundwater quality (North Spain). Water Research 42, 3315-3326.

Hornberger, G.M., Raffensperger, J.P., Wiberg, P.L., Eshleman, K.N., 1998. Open Chanel Hydraulics. In: Elements of Physical Hydrology. The Johns Hopkins University Press, Baltimore, 73-97.

Hutchins, P., Smith, E., K., Koepfler, E., Viso, R.F., Peterson, R.N., 2014. Metabolic responses of estuarine microbial communities to discharge of surface runoff and groundwater from contrasting landscapes. Estuaries and Coasts, 37 (3): 736-750.

Johnson, S.L., Sayre, D.M., 1973. Effects of urbanization on floods in the Houston, Texas metropolitan area. United State Geological Survey Water Resources Inventory, 3 (73): 50.

Lambert, M.J., Burnett, W.C., 2003. Submarine groundwater discharge estimates at a Florida coastal site based on continuous radon measurements. Biogeochemistry 66, 55-73.

Lautz, L.K., 2007. Estimating groundwater evapotranspiration rates using diurnal water-table fluctuations in a semi-arid riparian zone. Hydrogeology Journal, 16 (3): 483-497.

Lee, J., Kim, G., 2006. A simple and rapid method for analyzing radon in coastal and ground waters using a radon-in-air monitor. Journal of Environmental Radioactivity 89, 219-228.

Libes, S., Peterson, R., 2014. Briarcliffe Acres groundwater and lake level monitoring. http://bccmws.coastal.edu/bagw/index.html.

Loucaides, S., Cahon, L.B., Henry, E.J. 2007. Effects of watershed impervious cover on dissolved silica loading in storm flow. Journal of the American Water Resources Association, 43 (4): 841-849.

MacIntyre, S., Wanninkhof, R., Chanton, J.P., 1995. Trace gas exchange across the air–sea interface in freshwater and coastal marine environments. In: Matson, P.A., Harris, R.C. (Eds.), Biogenic Trace Gases: Measuring Emissions from Soil and Water. Blackwell Science Ltd, Boston, 52–97.

McCoy, C.A., Corbett, C.A., Cable, J.E., Spruill, R.K., 2007. Hydrogeological characterization of southeast coastal plain aquifers and groundwater discharge to Onslow Bay, North Carolina (USA). Journal of Hydrology 339, 159-171.

Meriano, M., Howard, K. W.F., Eyles, N. 2011. The role of midsummer urban aquifer recharge in stormflow generation using isotopic and chemical hydrograph separation techniques. Journal of Hydrology 396, 82-93.

Moore, W.S., Reide, D.F., 1973. Extraction of radium from natural waters using manganese-impregnated acrylic fibers. Journal of Geophysical Research 78, 8880-8886.

Mullinger, N.J., Binley, A.M., Pates, J.M., Crook, N.P., 2007. Radon in Chalk streams: Spatial and temporal variation of groundwater sources in the Pang and Lambourn catchments, UK. Journal of Hydrology 339, 172-182.

Mullinger, N.J., Pates, J.M., Binley, A.M., Crook, N.P., 2009. Controls on the spatial and temporal variability of ^{222}Rn in riparian groundwater in a lowland Chalk catchment. Journal of Hydrology 376, 58-69.

Paul, M.J., Meyer, J.L., 2001. Streams in the urban landscape. Annual Review of Ecology and Systematics, 32 (1): 333-365.

Peterson, R.N., Burnett, W.C., Dimova, N., Santos, I.R., 2009. A comparison of measurement methods for radium-226 on manganese-fiber. Limnology and Oceanography: Methods 7, 196-205.

Peterson, R.N., Santos, I.R., Burnett, W.C., 2010. Evaluating groundwater discharge to tidal rivers based on a Rn-222 time-series approach. Estuarine, Coastal and Shelf Science 86, 165-178.

Raffersperger, J.F., Cochrane, T.A., 2010. A smart market for impervious cover. Water Recourses Management, 24 (12) 3065-3083.

Ragab, R., Rosier, P., Dixon, A., Bromley, J., Cooper, J.D., 2003. Experimental study of water fluxes in a residential area: Road infiltration, runoff and evaporation. Hydrological Processes 17, 2423-2437. doi: 10.1002/hyp.1251.

Santos, I.R., Dimova, N., Peterson, R.N., Mwashote, B., Chanton, J., Burnett, W.C., 2009. Extended time series measurements of submarine groundwater discharge tracers (^{222}Rn and CH_4) at a coastal site in Florida. Marine Chemistry 113, 137-147.

Santos, I.R., Peterson, R.N., Eyre, B.D., Burnett, W.C., 2010. Significant lateral inputs of fresh groundwater into a stratified tropical estuary: Evidence from radon and radium isotopes. Marine Chemistry121, 37-48.

Schueler, T., 2000. Influence of groundwater on performance of stormwater ponds in Florida: The practice of watershed protection. Watershed Protection Techniques 2(4), 525-528.

Stringer, C.E., Burnett, W.C. 2004. Sample bottle design improvements for radon emanation analysis of natural waters. Health Physics 87, 642-646.

Swarzenski, P.W., 2007. U/Th series radionuclides as coastal groundwater tracers. Chemical Reviews 107(2), 663-674.

Vietz, G.J., Sammonds, M.J., Walsh, C.J., Fletcher, T.D., Rutherfurd, I.D., Stewardson, M.J., 2014. Ecologically relevant geomorphic attributes of streams are impaired by even low levels of watershed effective imperviousness. Geomorphology 206, 67-78.

Winter, 1999. Relation of streams, lakes, and wetlands to groundwater flow systems. Hydrogeology Journal, 7: 28-45.

Xue, J., Gavin, K., 2008. Effect of rainfall intensity on infiltration into partly saturated slopes. Geotechnical and Geological Engineering 26, 199-209.

Tables

Table 1. Dogwood Swash monthly average values for water budget parameters. Months containing less than 70% of the record have been excluded.

		Mean Total Discharge (m^3/s)	Mean Groundwater Discharge (m^3/s)	Mean Surface Runoff Discharge (m^3/s)	Mean Direct Precipitation Discharge (m^3/s)	Mean Groundwater Fraction (%)	Mean Surface Runoff Fraction (%)	Mean Direct Precipitation Fraction (%)
2012	January	$2.15 * 10^{-2}$	$1.34 * 10^{-3}$	$2.01 * 10^{-2}$	$2.50 * 10^{-7}$	6.46	93.54	$1.16 * 10^{-3}$
	February	$2.02 * 10^{-2}$	$1.53 * 10^{-3}$	$1.86 * 10^{-2}$	$6.57 * 10^{-7}$	6.98	93.02	$3.26 * 10^{-3}$
	March	$3.55 * 10^{-2}$	$2.96 * 10^{-3}$	$3.26 * 10^{-2}$	$2.14 * 10^{-7}$	7.67	92.33	$6.02 * 10^{-4}$
	April	$3.06 * 10^{-2}$	$2.54 * 10^{-3}$	$2.80 * 10^{-2}$	$6.99 * 10^{-7}$	8.17	91.82	$2.29 * 10^{-3}$
	May	$3.79 * 10^{-2}$	$3.37 * 10^{-3}$	$3.45 * 10^{-2}$	$2.43 * 10^{-6}$	8.41	91.58	$6.42 * 10^{-3}$
	June	$2.80 * 10^{-2}$	$2.34 * 10^{-3}$	$2.56 * 10^{-2}$	$7.34 * 10^{-7}$	8.28	91.72	$2.62 * 10^{-3}$
	August	$2.60 * 10^{-2}$	$1.50 * 10^{-3}$	$2.45 * 10^{-2}$	$1.77 * 10^{-6}$	3.85	96.15	$6.23 * 10^{-3}$
	September	$2.22 * 10^{-2}$	$6.53 * 10^{-4}$	$2.16 * 10^{-2}$	$3.66 * 10^{-7}$	2.94	97.06	$1.65 * 10^{-3}$
	October	$1.55 * 10^{-2}$	$6.46 * 10^{-4}$	$1.48 * 10^{-2}$	$2.71 * 10^{-7}$	4.27	95.73	$1.75 * 10^{-3}$
	November	$2.57 * 10^{-2}$	$1.05 * 10^{-3}$	$2.46 * 10^{-2}$	$6.87 * 10^{-7}$	4.04	95.96	$2.67 * 10^{-3}$
2013	January	$3.53 * 10^{-2}$	$1.71 * 10^{-3}$	$3.35 * 10^{-2}$	$2.22 * 10^{-7}$	4.86	95.14	$6.29 * 10^{-4}$
	February	$4.51 * 10^{-2}$	$2.45 * 10^{-3}$	$4.27 * 10^{-2}$	$1.78 * 10^{-6}$	5.18	94.82	$3.94 * 10^{-3}$
	March	$5.44 * 10^{-2}$	$3.21 * 10^{-3}$	$5.12 * 10^{-2}$	$1.10 * 10^{-6}$	5.80	94.20	$2.02 * 10^{-3}$
	April	$4.79 * 10^{-2}$	$3.70 * 10^{-3}$	$4.42 * 10^{-2}$	$3.69 * 10^{-6}$	7.51	92.48	$7.70 * 10^{-3}$
	May	$2.41 * 10^{-2}$	$1.84 * 10^{-3}$	$2.23 * 10^{-2}$	$3.57 * 10^{-7}$	6.40	93.60	$1.48 * 10^{-3}$
	June	$2.24 * 10^{-2}$	$5.58 * 10^{-4}$	$2.19 * 10^{-2}$	$1.44 * 10^{-6}$	2.56	97.44	$6.44 * 10^{-3}$
	July	$2.55 * 10^{-2}$	$5.91 * 10^{-4}$	$2.49 * 10^{-2}$	$7.10 * 10^{-7}$	2.24	97.75	$2.78 * 10^{-3}$

Table 2. Yearly mean values for all measured parameters. Percent change and differences were all calculated chronologically where positive values indicate an increase in the parameter of interest from 2012 to 2013 and negatives indicate a decrease. Reported yearly values represent data collected in January through June of each respective year.

	Mean Total Discharge (m^3/s)	Mean Groundwater Discharge (m^3/s)	Mean Surface Runoff Discharge (m^3/s)	Mean Direct Precipitation Discharge (m^3/s)	Mean Groundwater Fraction (%)	Mean Surface Runoff Fraction (%)	Mean Direct Precipitation Fraction (%)
2012	$2.89 * 10^{-2}$	$2.35 * 10^{-3}$	$2.66 * 10^{-2}$	$8.31 * 10^{-7}$	7.66	92.34	$2.72 * 10^{-3}$
2013	$3.64 * 10^{-2}$	$2.01 * 10^{-3}$	$3.44 * 10^{-2}$	$1.33 * 10^{-6}$	4.93	95.06	$3.57 * 10^{-3}$
% Change	25.81	-14.32	29.35	59.99	-35.60	2.95	31.07
Difference	$7.47 * 10^{-3}$	$3.36 * 10^{-4}$	$7.80 * 10^{-3}$	$4.98 * 10^{-7}$	-2.73	2.73	$8.47 * 10^{-4}$

Figures

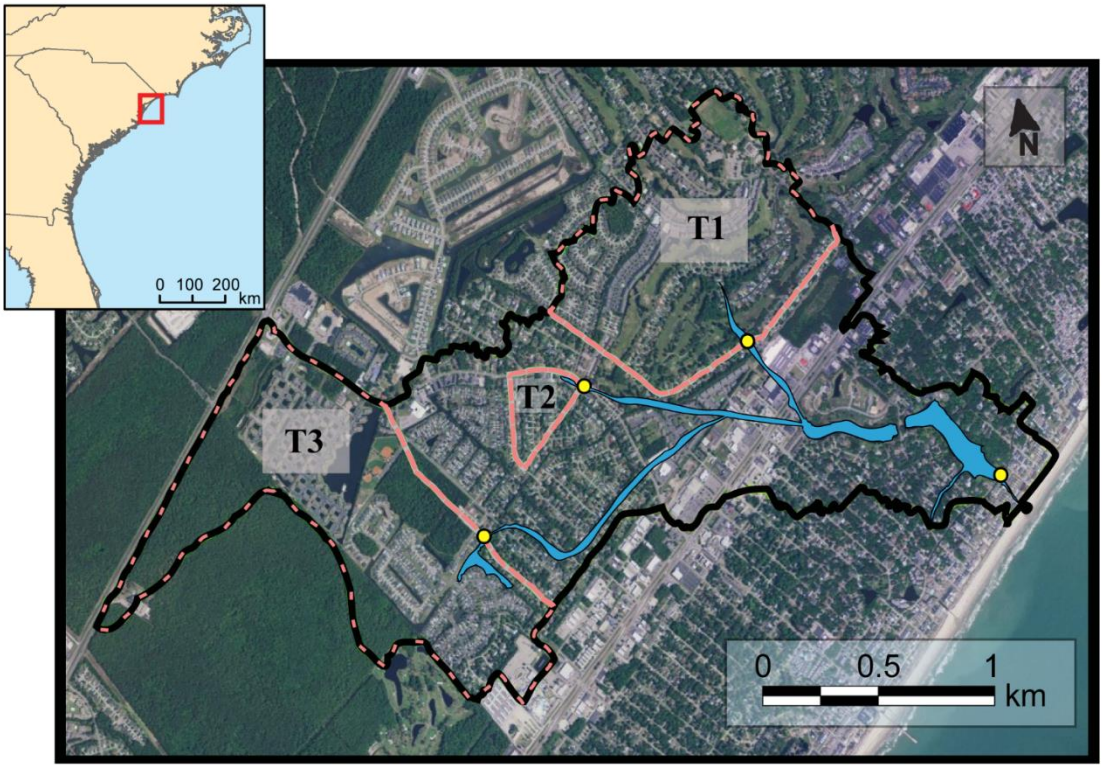

Figure 1. Dogwood Swash drainage basin (solid black line) and nested tributary sub-basins (dashed pink lines) with sampling locations (yellow dots). Dogwood Swash and upstream tributaries (T1, T2, and T3) represented by blue polygons. Tributary dimensions have been emphasized for illustrative purposes.

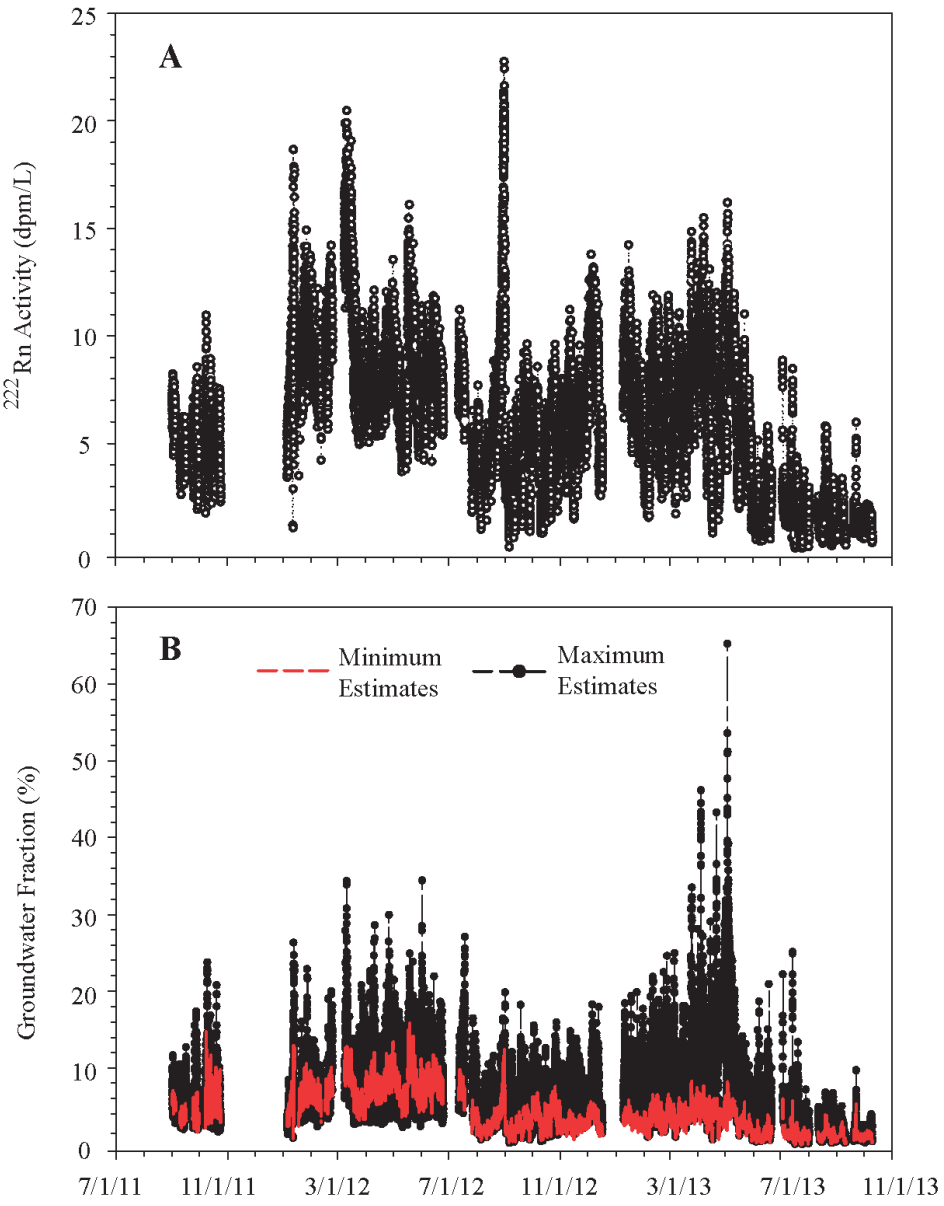

Figure 2. Observed high-resolution ^{222}Rn activities (A) and corresponding minimum and maximum percent groundwater fraction estimates (B) for Dogwood Swash.

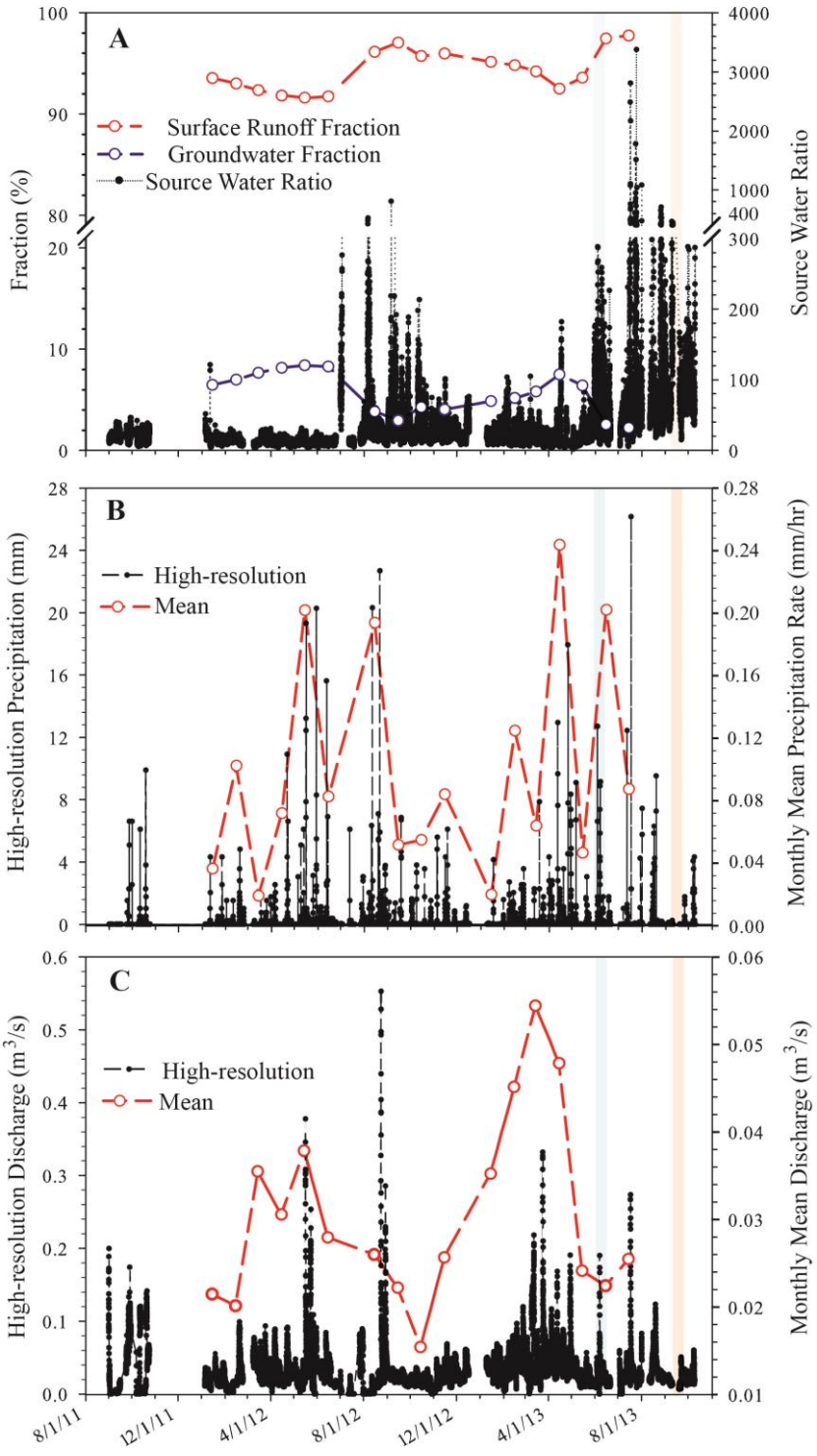

Figure 3. Monthly mean surface runoff and groundwater fractions with corresponding high-resolution source water ratios (surface runoff fraction/groundwater fraction) (A). Local high-resolution precipitation record with monthly mean precipitation rates (B). High-resolution total discharge rates from Dogwood Swash and monthly mean values (C). Semi-transparent orange and blue vertical bars represent data illustrated in Figures 7 and 8, respectively.

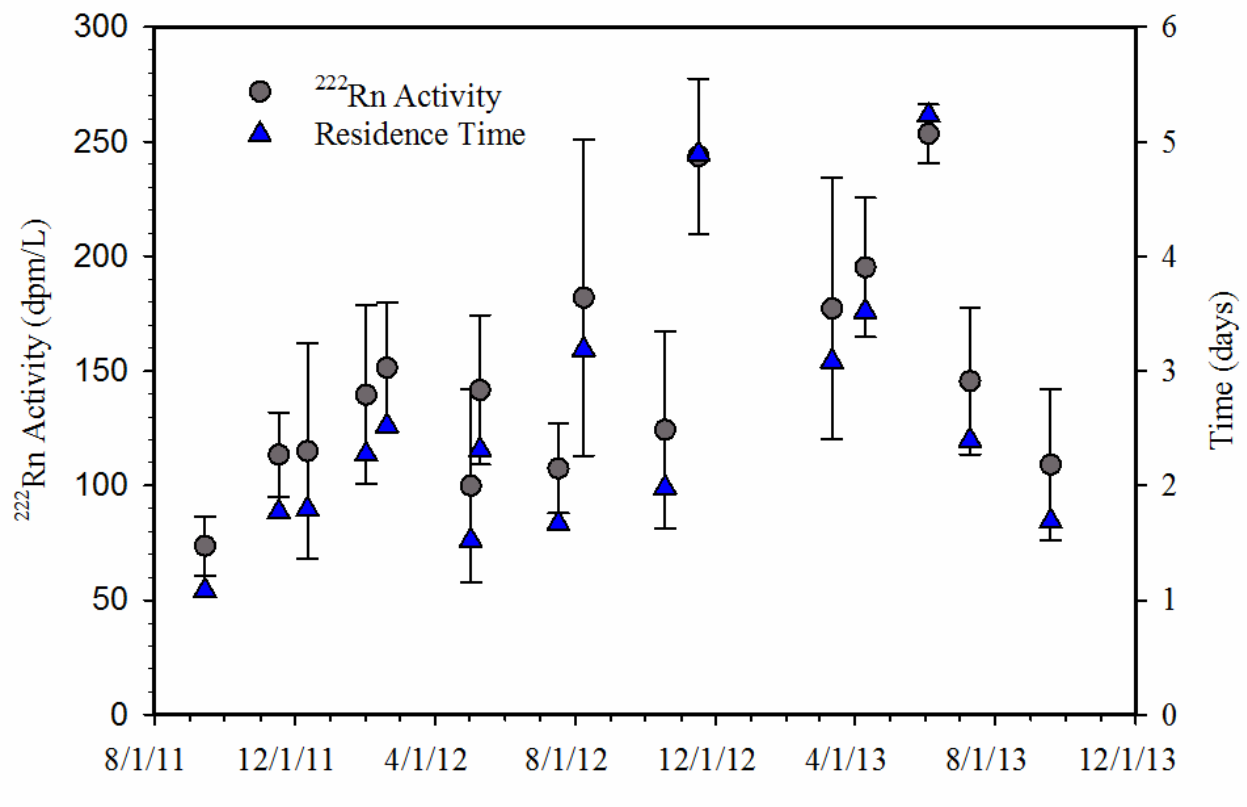

Figure 4. Mean groundwater end-member ^{222}Rn activities and corresponding groundwater residence times within the shallow aquifer. Averages represent data collected using piezometers installed at 0.5m, 1.0m, 1.25m, and 1.5m depths. Error bars represent 1-σ standard deviations.

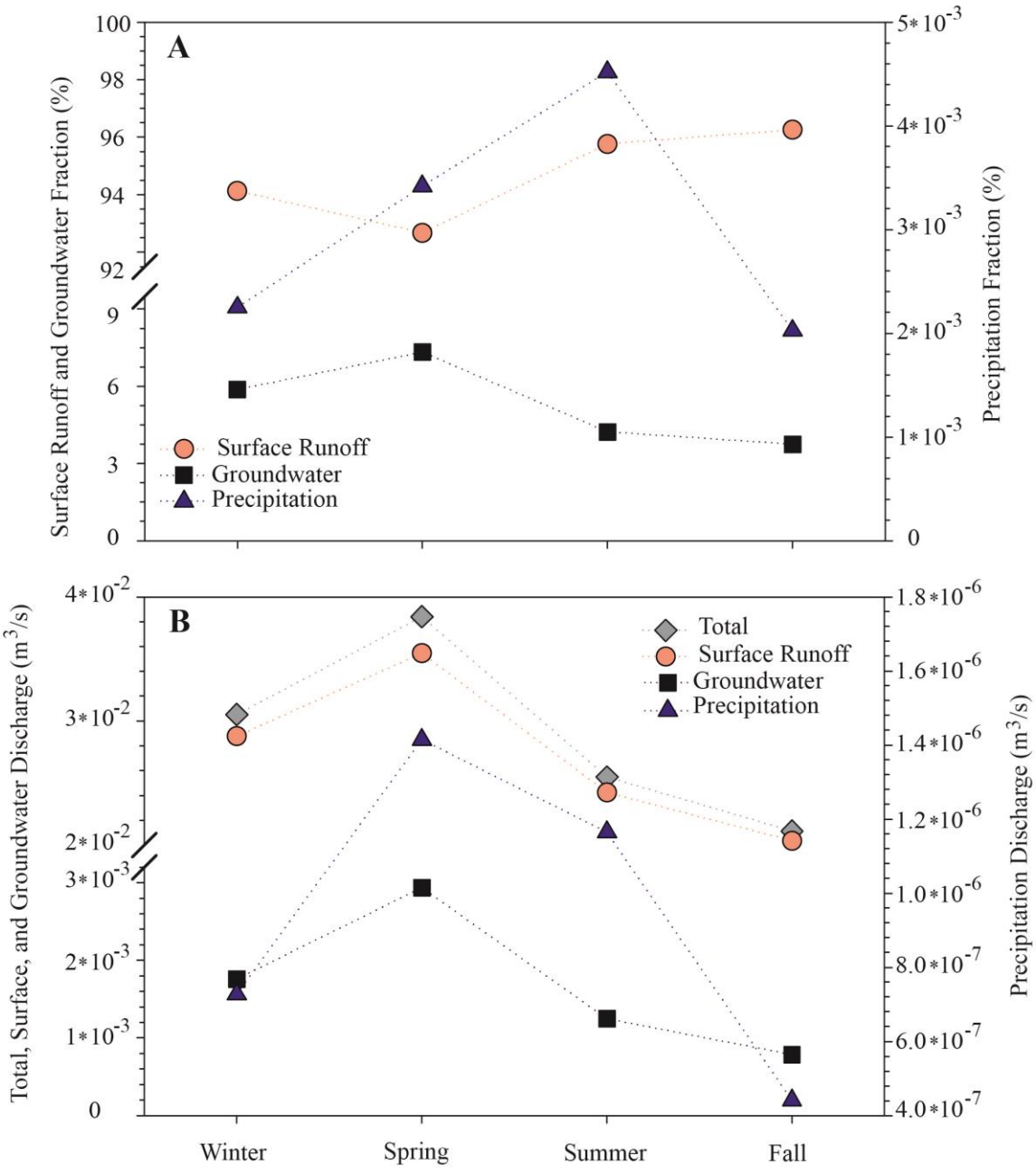

Figure 5. Seasonal averages of surface runoff, groundwater, and precipitation fractions in Dogwood Swash (A) and corresponding total, surface runoff, groundwater, and precipitation discharge rates (B).

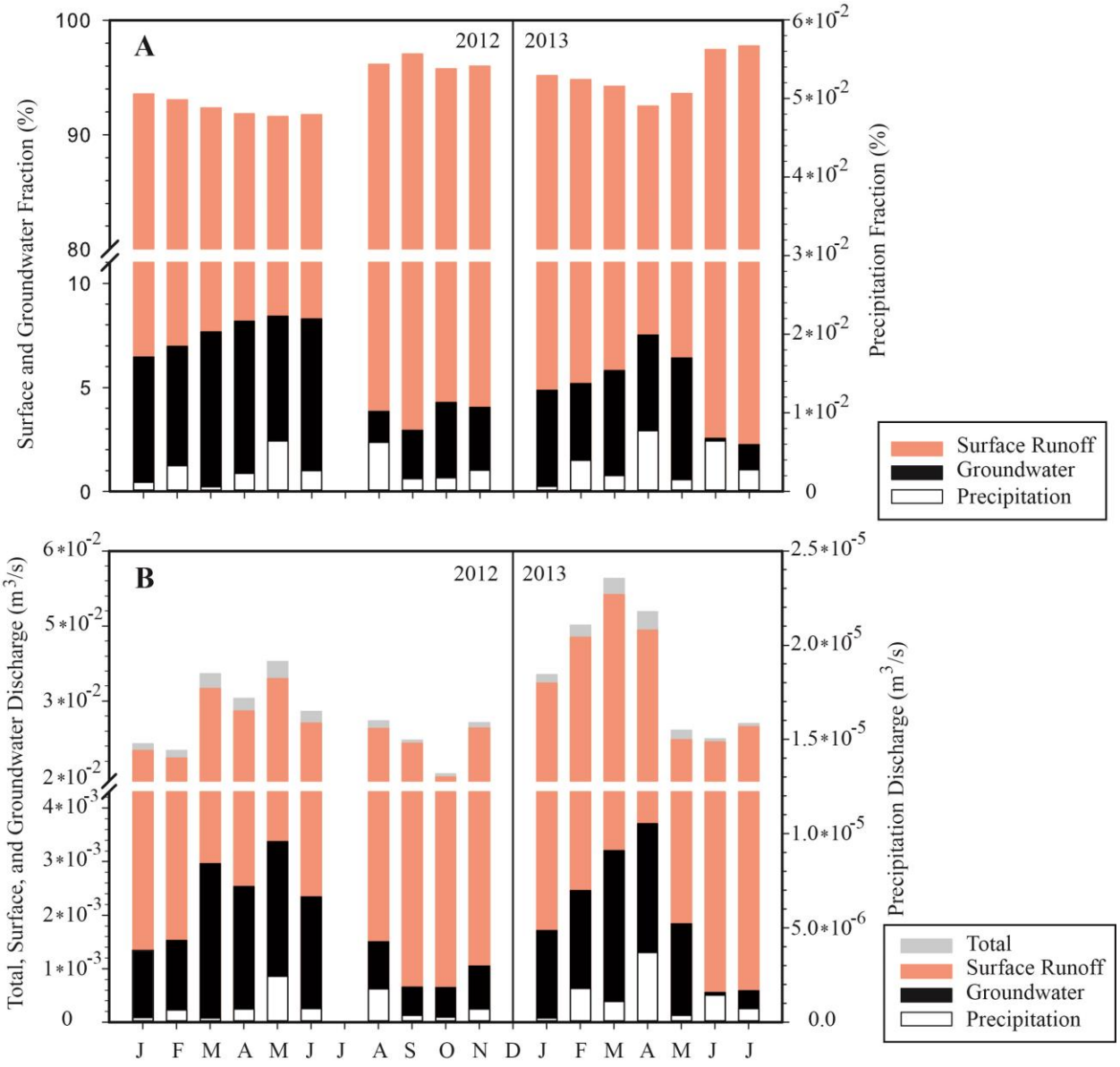

Figure 6. Monthly mean Dogwood Swash surface runoff, groundwater, and direct precipitation fractions (A) as well as total, surface runoff, groundwater, and precipitation discharge rates (B) from January 2012 through July 2013.

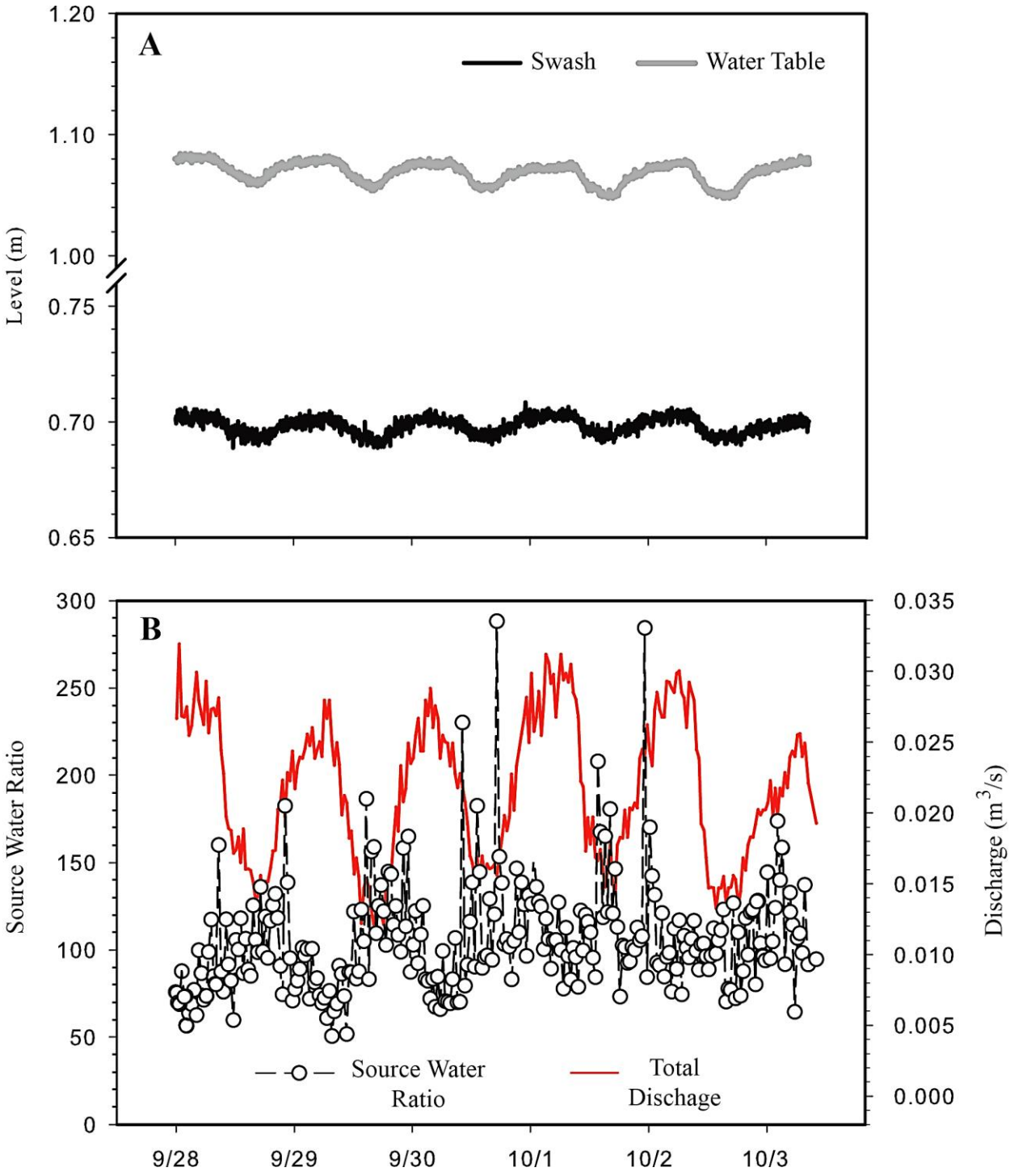

Figure 7. Dogwood Swash and local water table levels (A) with corresponding source water ratios and high-resolution total discharge rates (B) during six days of dry conditions in 2013.

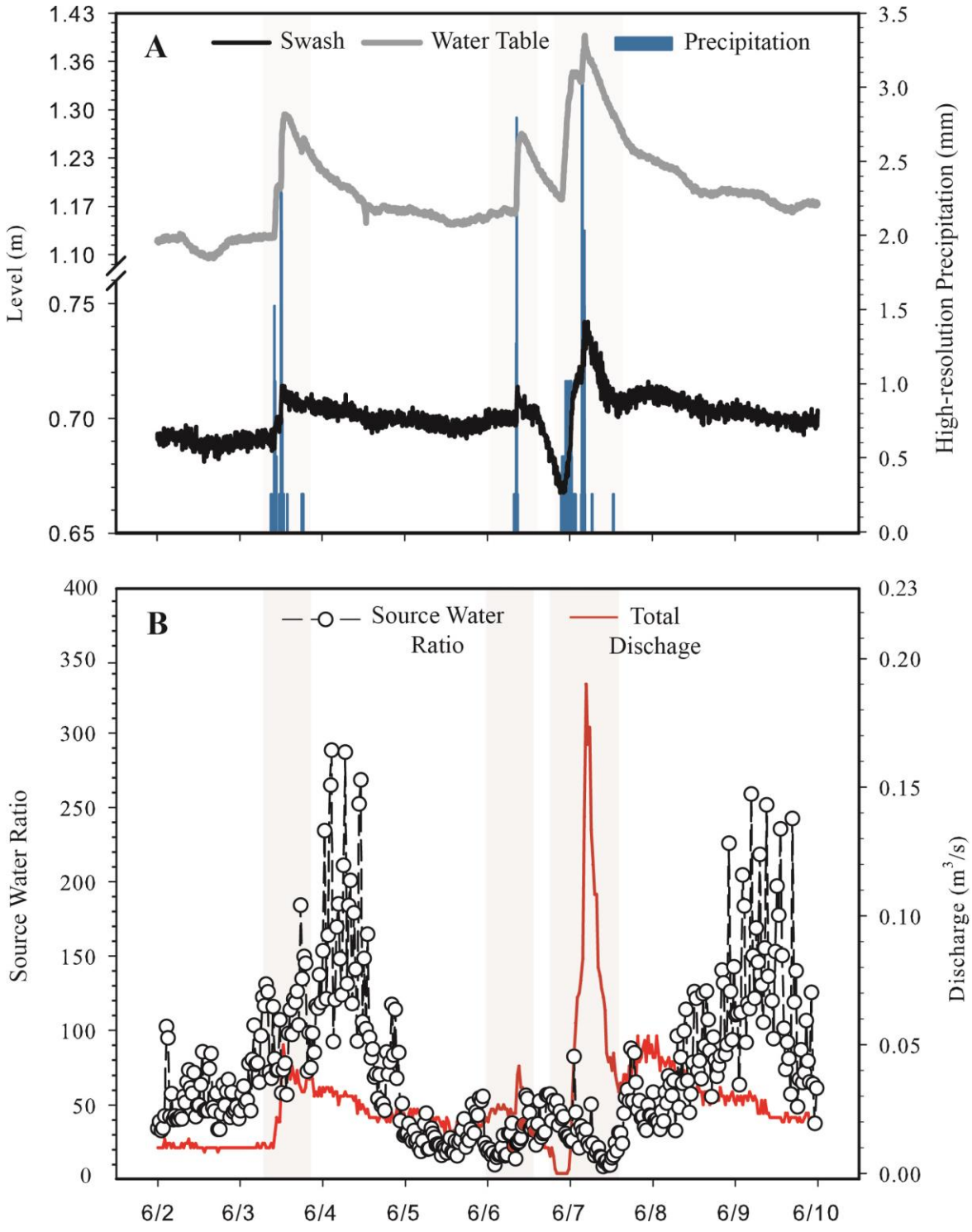

Figure 8. Dogwood Swash and local water table levels with high-resolution precipitation (A). Source water ratios and high-resolution total discharge rates (B) during three rainfall events (indicated by gray semi-transparent vertical bars) in June 2013.

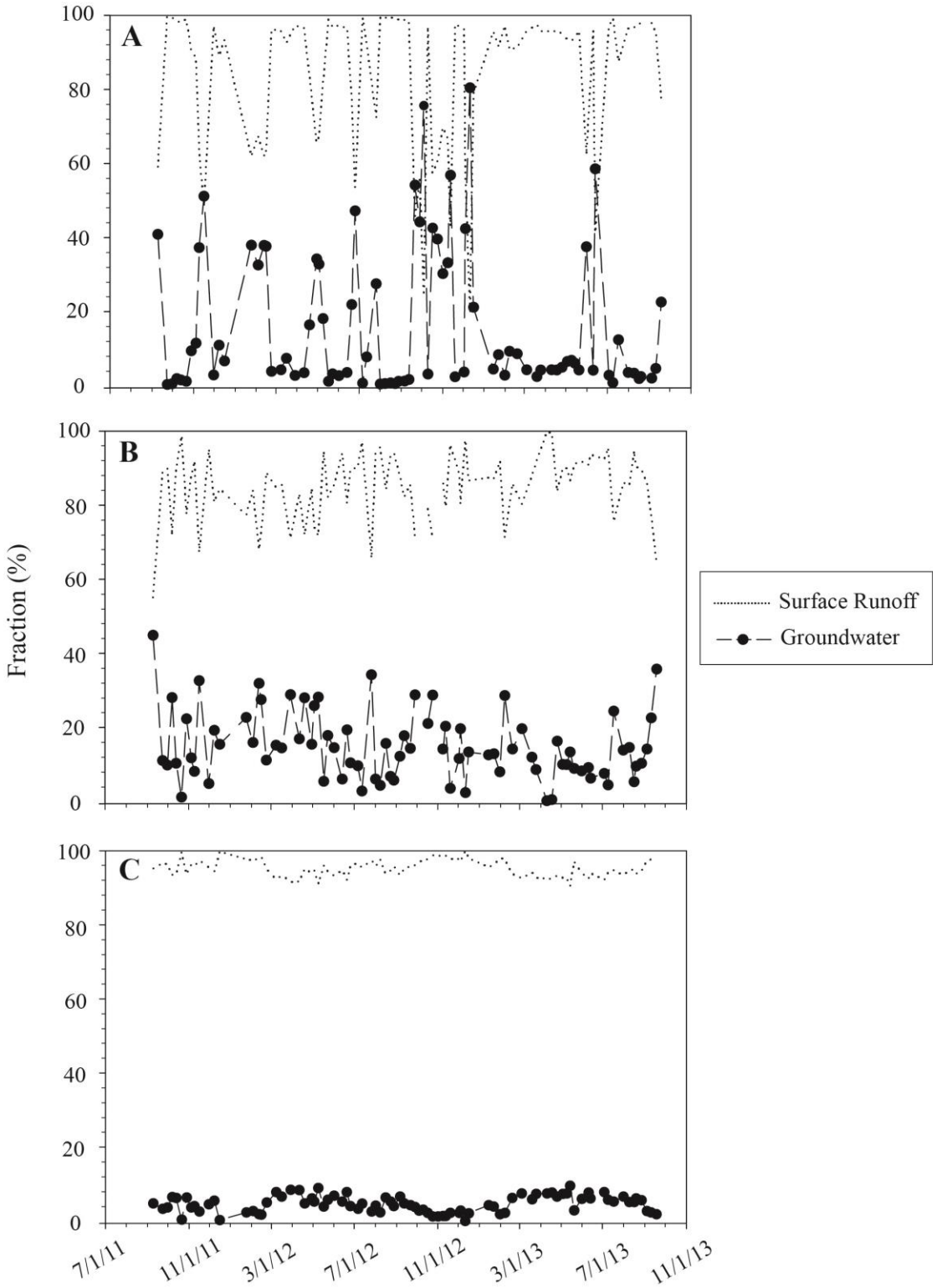

Figure 9. Surface runoff and groundwater fractions for T3 (A), T1 (B), and T2 (C) from September 2011 through September 2013. Panels (A through C) are arranged by increasing impervious cover where 48% of the T3 basin is impervious surface, 60% of the T1 basin is impervious surface, and 95% of the T3 basin is impervious surface.